

# DEMODULATION OF IMAGES MODELED BY AMPLITUDE-FREQUENCY MODULATIONS USING MULTIDIMENSIONAL ENERGY SEPARATION

Petros Maragos<sup>1</sup> and Alan C. Bovik<sup>2</sup>

<sup>1</sup>School of ECE, Georgia Institute of Technology, Atlanta, GA 30332, USA

<sup>2</sup>Department of ECE, The University of Texas, Austin, TX 78712, USA

## ABSTRACT

Locally narrowband images can be modeled as 2D spatial AM-FM signals with several applications in image texture analysis and computer vision. In this paper we formulate such an image demodulation problem, and present a solution based on the multidimensional energy operator  $\Phi(f) = \|\nabla f\|^2 - f\nabla^2 f$ . We discuss some interesting properties of this multidimensional operator and develop multidimensional energy separation algorithms to estimate the amplitude envelope and instantaneous frequencies of 2D spatially-varying AM-FM signals. Experiments are also presented on applying this 2D energy demodulation algorithm to estimate the instantaneous amplitude contrast and spatial frequencies of image textures bandpass filtered via Gabor filters. The attractive features of the multidimensional energy operator and the 2D energy separation algorithm are their simplicity, efficiency, and ability to track instantaneously-varying spatial modulation patterns.

## 1. INTRODUCTION

Image textures of the locally-narrowband type can be modeled as 2D spatial AM-FM signals

$$f(x, y) = a(x, y) \cos[\phi(x, y)] \quad (1)$$

that are 2D sines containing both amplitude modulation (AM) and frequency modulation (FM). Namely, they have a spatially varying amplitude  $a(x, y)$  and a spatially-varying instantaneous frequency vector  $\vec{\omega}(x, y) = \nabla\phi(x, y)$ . In particular, the amplitude  $a(x, y)$  is used to model local image contrast and the frequency vector contains rich information about the locally emergent spatial frequencies. Such modulation models have been proposed by Bovik et al. [1] and have been applied to a variety of image processing and vision problems. In Bovik et al. [1] and Havlicek et al. [2] these models are not applied directly to the whole (possibly wideband) image. Instead they are used on its bandpass filtered versions that are outputs from a filterbank consisting of 2D Gabor filters. The motivation in using Gabor filters is due to their attaining the lower limit of joint space-frequency resolution uncertainty and their ability to model early filtering stages of human vision [4].

P. Maragos' research was supported by the National Science Foundation under Grant MIP-9396301. A. Bovik's research was sponsored in part by the Air Force Office of Scientific Research, USAF, under grant F49620-93-1-0307.

An important problem in modeling image modulations with spatial AM-FM signals is to estimate the 2D amplitude and frequency signals using computational vision algorithms that have low complexity and small estimation error. In this paper we develop such an efficient approach for demodulation of 2D AM-FM signals based on a multidimensional energy operator introduced by Maragos, Bovik and Quatieri [7] and a related 2D energy separation algorithm. Our work has been inspired by a similar work for 1D signal and speech processing, where a 1D energy tracking operator [6] was used to develop a 1D energy separation algorithm [9] with applications to AM-FM signal and speech demodulation [8, 9]. In the 2D discrete case, the discretized energy operator we use is identical to the one developed in Yu, Mitra and Kaiser [11] for digital image edge detection, and also used in [10] for image enhancement.

## 2. 1D ENERGY OPERATOR AND ENERGY SEPARATION

In his work on nonlinear modeling of speech production, Teager developed a nonlinear differential operator  $\Psi_c$  for 1D continuous-time signals  $f(t)$ , defined as

$$\Psi_c(f)(t) \triangleq [f'(t)]^2 - f(t)f''(t) \quad (2)$$

where  $f' = df/dt$  and  $f'' = d^2f/dt^2$ . The discrete-time counterpart of  $\Psi_c$  is the operator

$$\Psi_d(f)(n) \triangleq f^2(n) - f(n-1)f(n+1) \quad (3)$$

for discrete-time signals  $f(n)$ . Both operators were first introduced systematically by Kaiser [5, 6].  $\Psi_c$  is an 'energy-tracking' operator because it can track the energy of simple harmonic oscillators that produce sinusoidal oscillatory signals; this energy is proportional to the product of the amplitude squared and frequency squared of the oscillation. Hence we shall refer to  $\Psi_c$  and  $\Psi_d$  as the 1D energy operators.

The energy operators are very efficient in instantaneously estimating the modulating signals of 1D AM-FM signals. Specifically, Maragos, Kaiser, and Quatieri [8, 9] have shown that the energy operators can approximately estimate the envelope of AM signals and the instantaneous frequency of FM signals. For 1D AM-FM signals

$$f(t) = a(t) \cos[\phi(t)] \quad (4)$$

they have also found that the energy operator tracks the energy product

$$\Psi[a(t)\cos(\phi(t))] \approx a^2(t)\omega^2(t) \quad (5)$$

where  $\omega(t) = d\phi(t)/dt$  is the instantaneous (angular) frequency. This approximate result is valid (i.e., the approximation error is negligible) if the time-varying amplitude  $a(t)$  and frequency  $\omega(t)$  do not vary too fast in time or too greatly compared with the carrier. Sufficient conditions for this are a small amount of modulation and the amplitude and frequency modulating signals to be bandlimited with bandwidths much smaller than the carrier frequency. Further, they also developed an *energy separation algorithm (ESA)* [9] that, by separating the energy product (5), fully demodulates the AM-FM signal and estimates both its amplitude envelope  $|a(t)|$  and instantaneous frequency  $\omega(t)$ . The 1D energy operator and the ESA have found many applications in speech processing and communications [8, 9, 3].

### 3. CONTINUOUS MULTIDIMENSIONAL ENERGY OPERATOR AND SEPARATION

Let  $f(\vec{x})$  be a  $\nu$ D real-valued signal with a continuous argument  $\vec{x} = (x_1, \dots, x_\nu) \in \mathbf{R}^\nu$ ,  $\nu = 2, 3, \dots$ . Then we define the  $\nu$ D energy operator by

$$\Phi_c(f)(\vec{x}) \triangleq \|\nabla f(\vec{x})\|^2 - f(\vec{x})\nabla^2 f(\vec{x}) \quad (6)$$

where  $\nabla f$  is the gradient of  $f$ ,  $\|\cdot\|$  is the Euclidean norm, and  $\nabla^2 f$  is the Laplacian of  $f$ . From its definition it follows directly that we can express  $\Phi_c(f)$  as

$$\Phi_c(f) = \sum_{k=1}^{\nu} \left( \frac{\partial f}{\partial x_k} \right)^2 - f \left( \frac{\partial^2 f}{\partial x_k^2} \right) = \sum_{k=1}^{\nu} \Psi_{c,k}(f) \quad (7)$$

where

$$\Psi_{c,k}(f) \triangleq \left( \frac{\partial f}{\partial x_k} \right)^2 - f \frac{\partial^2 f}{\partial x_k^2} \quad (8)$$

Thus the output of the  $\Phi_c$  is a *sum of 'energy components'*. Each energy component is the output of the 1D energy operator  $\Psi_c$  applied along each one of the  $\nu$  directions  $x_k$ . Hence, in analogy with the 1D case, we shall refer to  $\Phi_c$  as the '*multidimensional energy operator*'. Next we derive a few of its properties.

Let  $f(\vec{x})$  and  $g(\vec{x})$  be two  $\nu$ D signals. Applying  $\Phi_c$  to their product yields a similar result as in the 1D case. Specifically, since in general

$$\nabla(fg) = g\nabla f + f\nabla g \quad (9)$$

$$\nabla^2(fg) = g\nabla^2 f + f\nabla^2 g + 2(\nabla f) \cdot (\nabla g) \quad (10)$$

where ' $\cdot$ ' denotes inner product, it follows that

$$\Phi_c(fg) = f^2\Phi_c(g) + g^2\Phi_c(f) \quad (11)$$

For a multidimensional exponential signal, the output of the energy operator is identically zero:

$$\Phi_c[\exp\left(\sum_{k=1}^{\nu} c_k x_k\right)] = 0 \quad (12)$$

where  $c_k$  are arbitrary constants.

Applying  $\Phi_c$  to a  $\nu$ D cosine  $A \cos(\vec{\omega}_c \cdot \vec{x} + \theta)$  with constant phase offset  $\theta$ , constant amplitude  $A$ , and constant frequency vector  $\vec{\omega}_c = (\omega_{c,1}, \dots, \omega_{c,\nu})$  yields

$$\Phi_c[A \cos(\vec{\omega}_c \cdot \vec{x} + \theta)] = A^2 \left( \sum_{k=1}^{\nu} \omega_{c,k}^2 \right) = A^2 \|\vec{\omega}_c\|^2 \quad (13)$$

Consider the real-valued  $\nu$ D AM-FM signal

$$f(\vec{x}) = a(\vec{x}) \cos[\phi(\vec{x})] \quad (14)$$

where  $a(\vec{x})$  is a spatially-varying amplitude,  $\phi(\vec{x})$  is the phase signal,

$$\vec{\omega}(\vec{x}) \triangleq \nabla \phi(\vec{x}) = (\omega_1(\vec{x}), \dots, \omega_\nu(\vec{x})) \quad (15)$$

is the spatially-varying  $\nu$ D *instantaneous frequency vector*, and  $\omega_k(\vec{x})$  is the  $k$ -th instantaneous angular frequency signal. Assuming for each  $k$  that  $\omega_k$  is non-negative, we can always express it as

$$\omega_k(\vec{x}) = \omega_{c,k} + \omega_{m,k} q_k(\vec{x}) \quad (16)$$

where  $\omega_{c,k}$  is a constant center frequency,  $q_k(\vec{x}) \in [-1, 1]$  is the  $k$ -th frequency modulating signal, and  $\omega_{m,k}$  is the maximum deviation of  $\omega_k$  from its center value. Henceforth we assume that  $0 \leq \omega_{m,k} \leq \omega_{c,k}$ .

Applying  $\Phi_c$  to  $f$  yields

$$\Phi_c[a \cos(\phi)] = a^2 \|\vec{\omega}\|^2 - \frac{1}{2} a^2 \sin(2\phi) \nabla^2 \phi + \cos^2(\phi) \Phi_c(a) \quad (17)$$

For demodulation the desired term in (17) is  $a^2 \|\vec{\omega}\|^2$ . We view the rest of the terms as approximation error and show next that they are negligible under realistic assumptions.

Assume that  $a(\vec{x})$  is bandlimited in a circular frequency sphere of radius  $\omega_a$ . Namely, if  $A(\vec{u})$  is its  $\nu$ D Fourier transform, then  $A(\vec{u}) = 0$  for  $\|\vec{u}\| > \omega_a$ . Then if we define the mean spectral absolute value of  $a$  as

$$\mu_a = \frac{1}{(2\pi)^\nu} \int_{-\omega_a}^{\omega_a} \dots \int_{-\omega_a}^{\omega_a} |A(\vec{u})| du_1 \dots du_\nu \quad (18)$$

it can be shown that for each  $k$

$$|a(\vec{x})| \leq a_{max} \leq \mu_a, \quad \left| \frac{\partial a}{\partial x_k} \right| \leq \omega_a \mu_a, \quad \left| \frac{\partial^2 a}{\partial x_k^2} \right| \leq \omega_a^2 \mu_a$$

$$|\Phi_c(a)(\vec{x})| \leq 2\omega_a^2 \mu_a^2$$

where  $a_{max} = \sup_{\vec{x}} |a(\vec{x})|$ . Assume also that each frequency signal  $\omega_k(\vec{x})$  is bandlimited with bandwidth  $\omega_{q,k} < \omega_{c,k}$ . Then we can consider the approximation

$$\Phi_c[a \cos(\phi)] \approx a^2 \|\vec{\omega}\|^2 \quad (19)$$

with an approximation error

$$E(\vec{x}) = \Phi_c[a \cos(\phi)] - a^2 \|\vec{\omega}\|^2 \quad (20)$$

that is bounded by

$$|E(\vec{x})| \leq \left( 2\omega_a^2 + \frac{1}{2} \sum_{k=1}^{\nu} \omega_{m,k} \omega_{q,k} \mu_{q,k} \right) \mu_a^2 \quad (21)$$

since

$$\frac{\partial^2 \phi}{\partial x_k^2} = \omega_{m,k} \frac{\partial q_k}{\partial x_k} \quad (22)$$

Assuming that  $a_{m,x} \approx \mu_a$  (which is true with equality if  $a$  is a cosine or has linear Fourier phase), the realistic conditions

$$\omega_a \ll \min_k \omega_{c,k} \text{ and } \omega_{m,k} \omega_{q,k} \ll (\omega_{c,k})^2 \quad \forall k \quad (23)$$

make the maximum absolute value of the error  $E$  much smaller than the maximum absolute value of the desired term. Thus, under such conditions, the approximation (19) is valid in the sense that the relative error is  $\ll 1$ . Note that conditions (23) imply that the amplitude and frequency signals do not vary too fast in space or too greatly compared with the carriers.

Now let us apply  $\Phi_c$  to the partial derivatives

$$\frac{\partial f}{\partial x_k} = \frac{\partial a}{\partial x_k} \cos(\phi) - a \omega_k \sin(\phi) \quad (24)$$

Due to (23) the second term in  $\partial a / \partial x_k$  has a much larger order of magnitude of its maximum absolute value compared with the first term. Thus we approximate  $\partial f / \partial x_k \approx -a \omega_k \sin(\phi)$  and apply (19) to obtain

$$\Phi_c \left( \frac{\partial f}{\partial x_k} \right) \approx \Phi_c [a \omega_k \sin(\phi)] \approx a^2 \omega_k^2 |\bar{\omega}|^2 \quad (25)$$

for each  $k$ . Combining this equation and (19) yields

$$\sqrt{\frac{\Phi_c \left( \frac{\partial f}{\partial x_k} \right)}{\Phi_c(f)}} \approx \omega_k(\bar{x}), \quad k = 1, 2, \dots, \nu$$

$$\frac{\Phi_c(f)}{\sqrt{\sum_{k=1}^{\nu} \Phi_c \left( \frac{\partial f}{\partial x_k} \right)}} \approx |a(\bar{x})|$$

This algorithm can estimate at each location  $\bar{x}$  the amplitude envelope and instantaneous frequencies of the spatially-varying AM-FM signal. We call it the multidimensional *continuous energy separation algorithm (CESA)*. It is an extension of the 1D CESA developed in [9]. Note that, if  $f(\bar{x}) = A \cos(\bar{\omega}_c \cdot \bar{x} + \theta)$  is a pure cosine, then the CESA *exactly* estimates the constant amplitude  $a(\bar{x}) = |A|$  and constant frequency vector  $\bar{\omega} = \bar{\omega}_c$ .

#### 4. 2D DESA

In general, if we replace derivatives in  $\Phi_c$  with one-sample differences we obtain a discrete-space energy operator. For notational simplicity, we restrict our discussion to 2D signals, e.g., still images.

The alternative interpretation (7) of  $\Phi_c$  as a sum of energy components along different directions allows us to extend it to discrete-space signals  $f(m, n)$ . Specifically, replacing each of these energy components with outputs from 1D discrete-time energy operators  $\Psi_d$  yields the 2D discrete-space energy operator

$$\begin{aligned} \Phi_d(f)(m, n) &= \Psi_{d,1}(f)(m, n) + \Psi_{d,2}(f)(m, n) \\ &\triangleq 2f^2(m, n) - f(m-1, n)f(m+1, n) \\ &\quad - f(m, n-1)f(m, n+1) \end{aligned} \quad (26)$$

where the 1D energy operator

$$\Psi_{d,1}(f)(m, n) \triangleq f^2(m, n) - f(m-1, n)f(m+1, n)$$

applies horizontally on all rows of  $f$ , whereas  $\Psi_{d,2}$  operates on the columns. The above operator  $\Phi_d$  is identical to the one developed in [11, 10] for digital image edge detection for image enhancement.

Applying  $\Phi_d$  to a 2D sinusoid with constant amplitude/frequencies yields

$$\Phi_d[A \cos(\Omega_1 m + \Omega_2 n + \theta)] = A^2 [\sin^2(\Omega_1) + \sin^2(\Omega_2)] \quad (27)$$

Consider now a discrete AM-FM signal

$$f(m, n) = a(m, n) \cos[\phi(m, n)] \quad (28)$$

Its vertical instantaneous frequency (in radians/sample)

$$\Omega_1(m, n) \triangleq \frac{\partial \phi}{\partial m} = \Omega_{c,1} + \Omega_{m,1} q_1(m, n) \quad (29)$$

has center frequency  $\Omega_{c,1}$  and maximum frequency deviation  $\Omega_{m,1} \leq \Omega_{c,1}$ . The frequency modulating signal  $q_1(m, n)$  is assumed to be a mathematical function with a known computable integral. Likewise for the horizontal frequency  $\Omega_2 = \partial \phi / \partial n$ . All discrete-space frequencies are assumed to be in  $[0, \pi]$ . We henceforth assume that  $a$  is bandlimited with bandwidth  $\Omega_a$  and that both frequency signals are finite weighted sums of sinusoids and bandlimited with bandwidth  $\Omega_q$ . Then under the realistic assumptions

$$\Omega_a \ll \min_k \Omega_{c,k}, \quad \Omega_q \ll 1, \quad \Omega_{m,k} \ll \Omega_{c,k} \quad (30)$$

and by working as in [8], we obtain

$$\begin{aligned} \Phi_d[a(m, n) \cos(\phi(m, n))] &\approx \\ a^2(m, n) (\sin^2[\Omega_1(m, n)] + \sin^2[\Omega_2(m, n)]) \end{aligned} \quad (31)$$

Now replacing the partial derivatives of the previous section with *symmetric* 3-sample differences in each direction yields the 2D signals

$$\begin{aligned} g_1(m, n) &= [f(m+1, n) - f(m-1, n)]/2 \\ g_2(m, n) &= [f(m, n+1) - f(m, n-1)]/2 \end{aligned}$$

which are 2D AM-FM signals with amplitude and instantaneous frequencies that do not vary too fast or too much compared with the carriers  $\Omega_{c,k}$ . Hence (see also [9])

$$\Phi_d[g_1] \approx a^2 \sin^2[\Omega_1] (\sin^2[\Omega_1] + \sin^2[\Omega_2]) \quad (32)$$

$$\Phi_d[g_2] \approx a^2 \sin^2[\Omega_2] (\sin^2[\Omega_1] + \sin^2[\Omega_2]) \quad (33)$$

Combining (31), (32), (33) yields a *discrete energy separation algorithm (DESA)*

$$\begin{aligned} \arcsin \left( \sqrt{\frac{\Phi_d[f(m+1, n) - f(m-1, n)]}{4\Phi_d[f(m, n)]}} \right) &\approx \Omega_1(m, n) \\ \arcsin \left( \sqrt{\frac{\Phi_d[f(m, n+1) - f(m, n-1)]}{4\Phi_d[f(m, n)]}} \right) &\approx \Omega_2(m, n) \\ \sqrt{\frac{\Phi_d[f(m, n)]}{\sin^2[\Omega_1(m, n)] + \sin^2[\Omega_2(m, n)]}} &\approx |a(m, n)| \end{aligned} \quad (34)$$

The DESA can estimate at each location the amplitude envelope and two instantaneous frequency signals of a spatial AM-FM signal. Its constraint is that  $0 \leq \Omega_1, \Omega_2 \leq \pi/2$ ; i.e., it can estimate frequencies up to one fourth of the sampling frequency. The DESA in this paper is a 2D version of the 1D algorithm called 'DESA-2' in [9].

If the AM-FM signal has *constant* amplitude  $A$  and constant frequencies  $\Omega_{c,1}$  and  $\Omega_{c,2}$ , then the DESA equations provide an *exact* estimate of the amplitude  $|a(m, n)| = |A|$  and frequencies  $\Omega_1(m, n) = \Omega_{c,1}$  and  $\Omega_2(m, n) = \Omega_{c,2}$ .

Figure 1 shows the application of the 2D energy operator and DESA on a synthetic 2D AM-FM signal. The rms estimation error for the amplitude signal estimation, normalized by the rms of the true amplitude, was 0.0216. The relative rms errors for the estimated frequency signals were 0.0473 and 0.0429. We see that, as the theory predicts, the DESA can estimate the instantaneous amplitude and frequency signals of a spatial AM-FM signal (that had 50% AM and 20% FM) with very small estimation error, and with a very low computational complexity.

## 5. IMAGE DEMODULATION

The basic assumption behind the ability of the discrete or continuous ESA to demodulate 2D AM-FM signals, is that the signal is narrowband. This then prohibits its application to wideband images. A better strategy is to bandpass filter the image and apply the DESA to its narrowband components, assuming these are well modeled by spatial AM-FM signals. As bandpass filters we use 2D Gabor filters of the wavelet type, designed in [1] as a 2D radially symmetric filterbank. Each Gabor filter has a one octave bandwidth measured radially between the half-peak points.

Figure 2 shows the application of the 2D energy operator and DESA on Gabor bandpass filtered texture image. From this and other similar real image experiments we have observed the following: The energy operator acting on the original image enhances its contrast. Note that the energy operator may yield several negative values when applied to a wideband image as in Fig. 2(a). However, when applied to the narrowband (Gabor filtered) image of Fig. 2(c) it rarely yields negative values. The DESA can yield realistic estimates of the spatial instantaneous frequency signals, which can be more easily observed when shown as frequency vectors as in Fig. 2(h); there we see that the direction of the frequency vectors is most often perpendicular to the local waves in the image. However, there are also several outlier estimates, which are mostly caused by instantaneous numerical singularities of the DESA, e.g., when dividing by a very low energy value. These cause spikes in the DESA estimated amplitude and frequency signals which can be effectively filtered out by a 2D median filter. Finally, the amplitude signal seems to convey similar information as the energy operator output, mainly of the contrast type.

In conclusion, given that many locally narrowband image textures can be modeled by spatial AM-FM models and the ability of the DESA to efficiently estimate the slowly-varying amplitude and frequency signals, the 2D energy operator and 2D DESA become important tools for image analysis and computational vision.

## Acknowledgement

We wish to express our gratitude to Joe Havlicek at the University of Texas, Austin, for producing sets of bandpass filtered images through a 2D Gabor filterbank.

## 6. REFERENCES

- [1] A. C. Bovik, N. Gopal, T. Emmoth, and A. Restrepo, "Localized measurement of Emergent Image Frequencies by Gabor Wavelets", *IEEE Trans. Info. Theory*, IT-38, pp. 691-712, Mar. 1992.
- [2] J. P. Havlicek, A. C. Bovik, and P. Maragos, "Modulation Models for Image Processing and Wavelet-based Image Demodulation", in *Proc. 26th Annual Asilomar Conf. on Signals, Systems and Computers*, Monterey, CA, Oct. 1992.
- [3] A. C. Bovik, P. Maragos, and T. F. Quatieri, "AM-FM Energy Detection and Separation in Noise Using Multi-band Energy Operators", *IEEE Trans. Signal Processing*, vol. 41, pp. 3245-3265, Dec. 1993.
- [4] J. E. Daugman, "Uncertainty relation for resolution in space, spatial frequency, and orientation optimized by two-dimensional visual cortical filters", *J. Opt. Soc. Amer. A*, vol. 2(7), pp. 1160-1169, July 1985.
- [5] J. F. Kaiser, "On a simple algorithm to calculate the 'energy' of a signal", in *Proc. IEEE Int'l. Conf. Acoust., Speech, Signal Processing*, Albuquerque, NM, pp. 381-384, April 1990.
- [6] J. F. Kaiser, "On Teager's Energy Algorithm and Its Generalization to Continuous Signals", in *Proc. IEEE Digital Signal Processing Workshop*, Mohonk (New Paltz), NY, Sep. 1990.
- [7] P. Maragos, A. C. Bovik, and T. F. Quatieri, "A Multidimensional Energy Operator for Image Processing", *Proc. SPIE vol 1818: Visual Communications and Image Processing '92*, pp. 177-186, Boston, Nov. 1992.
- [8] P. Maragos, J. F. Kaiser, and T. F. Quatieri, "On Amplitude and Frequency Demodulation Using Energy Operators", *IEEE Trans. Signal Processing*, vol. 41, pp. 1532-1550, April 1993.
- [9] P. Maragos, J. F. Kaiser, and T. F. Quatieri, "Energy Separation in Signal Modulations with Application to Speech Analysis", *IEEE Trans. Signal Processing*, vol. 41, pp. 3024-3051, Oct. 1993.
- [10] S. K. Mitra, H. Li, I.-S. Lin, and T.-H. Yu, "A New Class of Nonlinear Filters for Image Enhancement", in *Proc. IEEE Int'l Conf. Acoust., Speech, Signal Processing*, pp. 2525-2528, Toronto, Canada, May 1991.
- [11] T.-H. Yu, S. K. Mitra, and J. F. Kaiser, "Novel Algorithm for Image Enhancement", in *Proc. SPIE/SPSE Conf. on Image Processing Algorithms and Techniques II*, San Jose, CA, Feb. 1991.

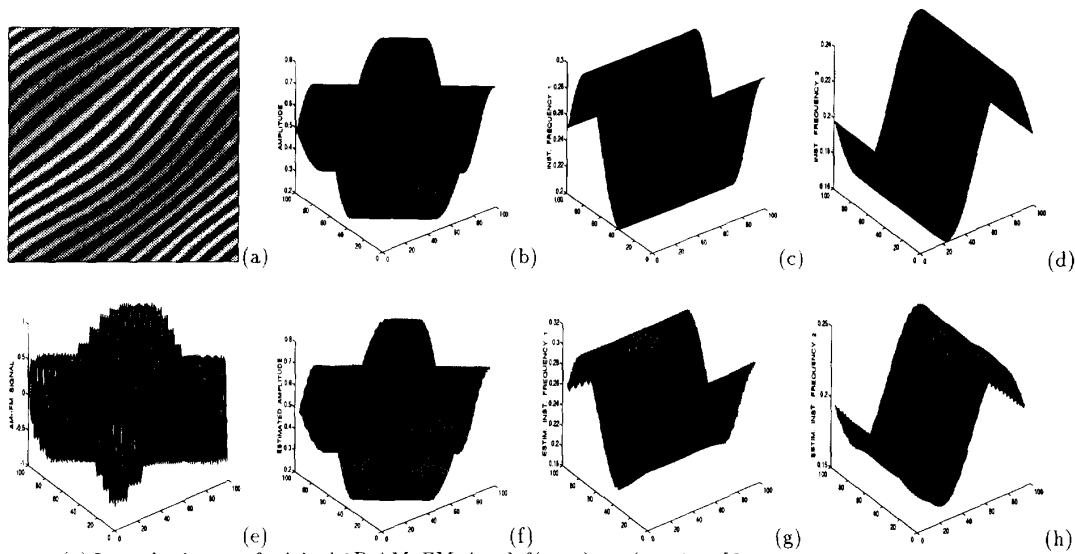


Figure 1. (a) Intensity image of original 2D AM-FM signal  $f(m, n) = a(m, n) \cos[\Omega_1 m + \Omega_2 n + 2 \sin(\Omega_{q,1} m) + \sin(\Omega_{q,2} n + \frac{\pi}{2})]$ , where  $a(m, n) = 0.5[1 + 0.5 \cos(\Omega_{q,1} m + \Omega_{q,2} n)]$ ,  $\Omega_1 = \pi/4$ ,  $\Omega_2 = \pi/5$ , and  $m, n = 1, \dots, 100$ . (b) Original amplitude  $a$ . (c) Original frequency  $\Omega_1/\pi$ . (d) Original frequency  $\Omega_2/\pi$ . (e) Perspective plot of original image  $f$ . (f) Estimated amplitude via DESA. (g) Estimated frequency  $\Omega_1/\pi$  via DESA. (h) Estimated frequency  $\Omega_2/\pi$  via DESA.

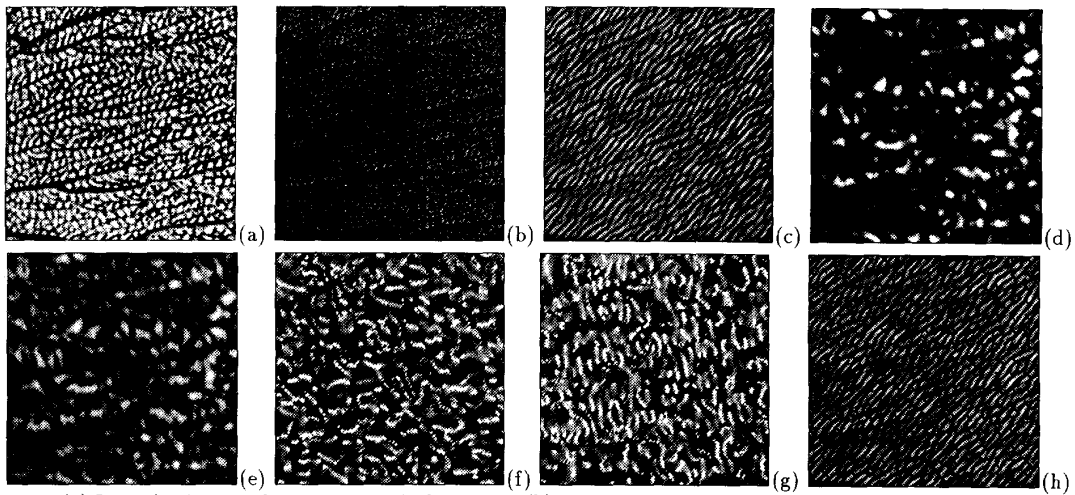


Figure 2. (a) Intensity image of a  $256 \times 256$ -pixel texture. (b) Output of energy operator on original image. (c) Bandpass filtered image via a Gabor filter whose horizontal and vertical center frequencies were (27, 27) cycles per image. (d) Output of energy operator on bandpass image. (e) Estimated amplitude via DESA. (f) Estimated frequency  $\Omega_1$  via DESA. (g) Estimated frequency  $\Omega_2$  via DESA. (h) Bandpass image with decimated frequency vectors  $(\Omega_1, \Omega_2)$  superimposed (in black and amplified in magnitude by 8). All image plots are normalized so that intensities are in  $[0, 255]$ .